Polymer Pen Lithography with Lipids for Large-Area Gradient Patterns

*Ravi Kumar,[†,§] Ainhoa Urtizberea,[†] Souvik Ghosh,[†,‡] Uwe Bog,[†] Quinn Rainer,[∥] Steven Lenhert,[∥] Harald Fuchs,[†,§] and Michael Hirtz *[,†]*

AUTHOR ADDRESS

[†]Institute of Nanotechnology (INT) and Karlsruhe Nano Micro Facility (KNMF), Karlsruhe Institute of Technology (KIT), 76131 Karlsruhe, Germany

[‡]Sardar Vallabhbhai National Institute of Technology (SVNIT), Surat, Gujarat 395007, India

[§]Physical Institute and Center for Nanotechnology (CeNTech), University of Münster, 48149 Münster, Germany

[∥]Florida State Univ, Dept Biol Sci and Integrat NanoSci Inst, Tallahassee, Florida 32306 United States

ABSTRACT

Gradient patterns comprising bioactive com-pounds over comparably (in regard to a cell size) large areas are key for many applications in the biomedical sector, in particular, for cell screening assays, guidance, and migration experiments. Polymer pen lithography (PPL) as an inherent highly parallel and large area technique has a great potential to serve in the fabrication of such patterns. We present strategies for the printing of functional phospholipid patterns via PPL that provide tunable feature size and feature density gradients over surface areas of several square millimeters. By controlling the printing parameters, two transfer modes can be achieved. Each of these modes leads to different feature morphologies. By increasing the force applied to the elastomeric pens, which increases the tip−surface contact area and boosts the ink delivery rate, a switch between a dip-pen nanolithography (DPN) and a microcontact printing (μCP) transfer mode can be induced. A careful inking procedure ensuring a homogeneous and not-too-high ink-load on the PPL stamp ensures a membrane-spreading dominated transfer mode, which, used in combination with smooth and hydrophilic substrates, generates features with constant height, independently of the applied force of the pens. Ultimately, this allows us to obtain a gradient of feature sizes over a mm^2 substrate, all having the same height on the order of that of a biological cellular membrane. These strategies allow the construction of membrane structures by direct transfer of the lipid mixture to the substrate, without requiring previous substrate functionalization, in contrast to other molecular inks, where structure is directly determined by the printing process itself. The patterns are demonstrated to be viable for subsequent protein binding, therefore adding to a flexible feature library when gradients of protein presentation are desired.

INTRODUCTION

Bioactive patterns with different feature densities or feature sizes play an important role in the investigation of molecular processes of cells growing on these patterns.[1−9] Furthermore, protein patterns are crucial for screening assays, e.g., in drug discovery,[10] and ordered large area arrangements of bio-molecules are crucial for development and applications in biocatalysis.[11−13] Large area patterns comprising gradients can allow parallel assays, screening the influence of pattern and feature design (shape, density, and size) for a biomaterial that exerts control over the cells' interaction, growth, differentiation, and/or proliferation over a wide

parameter range within one experiment.[4,14] Therefore, the material and time spent on individual experiments for the monitoring of cell response over the different density arrays can be avoided. Moreover, this approach provides similar environmental conditions for all parameters tested in parallel and increases the experimental throughput.[15] Additionally, gradient patterns over larger areas are crucial in cell guidance experiments[5] and migration assays. Overall, the substrate interface is of great importance in cell culture applications,[16] and lipids in particular can be effectively used as a biomimetic cell interface.[17] Therefore, patterning of lipids into gradient patterns becomes especially appealing for these kinds of applications.

Polymer pen lithography (PPL)[18] was introduced as a massively parallelized hybrid of dip-pen nanolithography (DPN)[19] and microcontact printing (μCP).[20] PPL utilizes the high-precision spatial control gained from the DPN setups with μCP like polymer stamps consisting of 2D arrays of pyramidal features in the tens of thousands on a square centimeter.[21] DPN and PPL are both capable of multiplexing, i.e., the deposition of more than one component in parallel and within one surface pattern.[3,22−28] The mild process parameters make the techniques especially interesting for printing biological materials, and in particular, DPN with phospholipids (L-DPN)[29] spawned many applications ranging from functionalization of sensor structures,[30] graphene,[31,32] and optical circuitry[33] to use in the biomedical context of research on allergy.[3,34,35] While L-DPN has already found various applications,[36] there are only a few studies on printing lipids via PPL, where it was used to demonstrate multicolor printing[26] or for quantum dot printing.[37] After transfer, the phospholipid inks self-assemble into orderly biomimetic membrane struc-tures.[38] Ink transport in L-DPN is governed by a complex balance between diffusion through the meniscus and on the surface driven by concentration differences at the tip/meniscus and meniscus/substrate interfaces.[39] Much less is known about the ink transfer process in printing lipids via PPL.[40] Intuitively, one can see PPL as a hybrid combination of μCP and DPN. In contrast to force-independent DPN, now the elastomeric tips provide an additional control parameter on feature size and shape upon changing the applied stamping force through z-piezo extension.[18,41] With more pen compression onto the substrate, a larger contact area of ink source is available,[21] and increasing the size of the ink source in DPN increases the flow rate.[42] Also, incrementing compression of the pens is expected to change the size of the condensed meniscus,[43−45] or the meniscus of hydrated lipids,[39,46] respectively, thereby further influencing the ink transport.[47,48] Particularly, in the case of lipid inks, the size and structure of the lipid molecules prevent diffusion of ink into the PPL stamp as observed for thiol based inks,[49] and homogeneous patterning with negligible ink depletion over time was reported.[26]

In PPL, feature size gradients can be introduced by tilting the PPL stamp in relation to the substrate,[50] while feature density gradients can be generated even with a homogeneously spaced tip array by applying a writing strategy as usually used in PPL multicolor patterning.[26,28] Both approaches are schematically shown in Scheme 1.

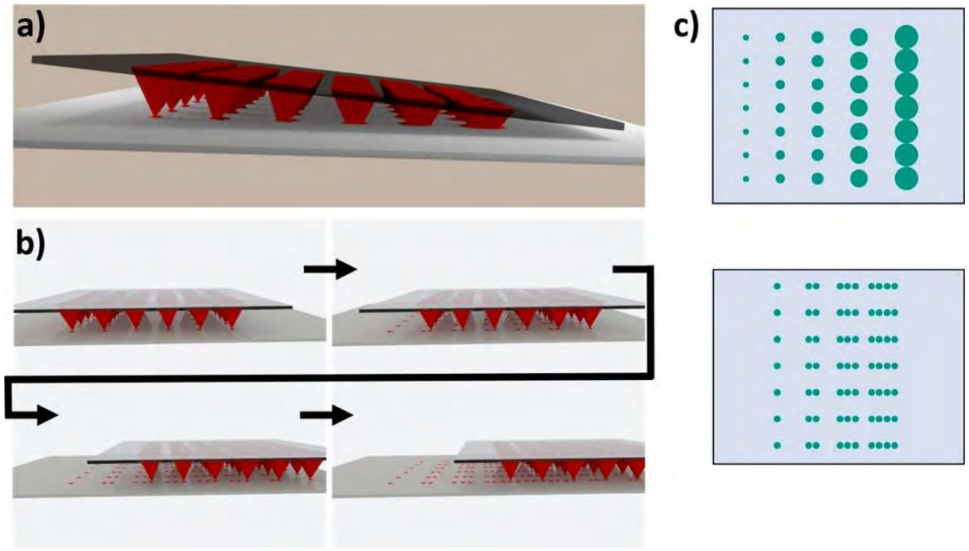

Scheme 1. (a) Scheme of a tilted pen array for generation of feature size gradients, (b) writing procedure with a levelled (parallel to substrate) pen array to achieve feature density gradients, and (c) resulting patterns of the processes depicted in (a) and (b), respectively, a features size gradient (top) and feature density gradient (bottom).

In the following, we will demonstrate both approaches in printing with phospholipid inks to generate size and density gradients of biomimetic lipid membrane stacks. Furthermore, we observe two distinct transfer modes for PPL with phospholipids that are controlled by the inking procedure, the interplay of smoothness and hydrophilicity of the substrate, and the amount of pressure applied to the stamp. The stability of the resulting patterns for applications in liquid is demonstrated by binding of protein to lipid features with specific binding sites.

EXPERIMENTAL

Phospholipids. All phospholipids employed in our experiments were obtained dissolved in chloroform from Avanti Polar Lipids, USA, and used as received. In this study, we have chosen as model ink 1,2-dioleoyl-sn-glycero-3-phosphocholine (DOPC), a well-known standard lipid for unsaturated lipid bilayer membranes, and widely employed as a lipid ink carrier in lipid mixtures. Being in the Lα liquid state in ambient conditions when hydrated, this amphiphilic ink allows full control of its diffusion, and therefore transport, by relative humidity under ambient conditions.[51,52] The 20 mg/mL (25.4 mM) solution of DOPC was mixed either with 1 mol % of the fluorescently labeled phospholipid 1,2-dioleoyl-sn-glycero-3-phosphoethanolamine-N-(liss-amine rhodamine B sulfonyl) (Liss Rhod PE) to facilitate detection of the lipid membranes by fluorescence microscopy or 5 mol % of 1-(12-biotinyl(aminododecanoyl))-2-oleoyl-sn-glycero-3-phosphoetha-nolamine (Biotin PE) for the generation of patterns used in protein binding experiments.

Substrates. Two types of substrates were employed for the experiments, SiO_2 SURFs and glass. SiO_2 SURFs substrates (type “standard SiO_2 SURF”, Nanolane, France) were used in order to analyze membrane structuration and spreading, as they are hydrophilic and optimized for surface enhanced ellipsometric contrast (SEEC) measurements (c.f., Optical Microscopy

section). SiO_2 SURFs comprise a layer system evoking the contrast enhancement with a top layer of hydrophilic rendered silicon oxide layer (see Supporting Information Figure S1). As the outermost layer of the SiO_2 SURFs is hydroxylated silicon oxide, these substrates behave in regard to surface chemistry similar to conventional, hydroxylated polished glass or hydroxylated silicon oxide surfaces.[38] For the experiments, the SiO_2 SURFs protective covers were peeled and the surfaces used as is for the printing experiments. The glass substrates (standard coverslips, VWR, Germany) were cleaned by ultrasonication, submerged for 10 min in chloroform, then for an additional 10 min in isopropanol and finally for 10 min in ultrapure water. After sonication, the substrates were dried under a nitrogen flow and used for the printing experiments.

PPL Stamp Fabrication. The PPL pen arrays were prepared according to procedures as described in the literature.[53] The hard PDMS polymer solution was prepared by mixing 3.4 g of vinyl-compound-rich prepolymer (ABCR, Karlsruhe), 18 μL of 2,4,6,8-tetramethyltetravinylcyclotetrasiloxane (Sigma-Aldrich, Germany) and one drop of platinum catalyst (platinum divinyltetramethyl disiloxane complex in xylene, Gelest, USA). The polymer solution was stirred in a falcon tube and put in a desiccator at low pressure (0.8 bar) for 1 h to degas. An amount of 0.8 g (25−35% methylhydrosiloxane)-dimethylsiloxane copolymer (ABCR, Karlsruhe) cross-linker was then mixed into the h-PDMS solution, stirred, degassed again, and poured onto the silicon master comprising the pyramidal array structure. Standard microscopic glass slides (VWR, Germany) were cut to pieces slightly bigger than the stamp sizes in the Si-master. The glass slides were carefully placed on the filled master and pressed down to fill the inverted pyramids of the Si-master homogeneously and to remove remaining air bubbles. The PDMS polymer was cured overnight on a hot plate at 72 °C. Then, the residual PDMS was carefully removed from the side of glass and the stamp array was detached from the master by using a scalpel.

Printing Process. All patterns were written with a NLP 2000 system (NanoInk, USA). Immediately before inking, stamps were treated with oxygen plasma (0.2 mbar, 100 W, 10 sccm O_2, 2 min, ATTO system, Diener electronics, Germany) to render the surface hydrophilic. The stamps were inked either by applying a 2 μL droplet of phospholipid ink directly to the stamp array with a pipet and drying with a nitrogen flow (in the overloading experiments) or (for the regular experiments) by spin-coating the same amount (30 s at 3500 rpm) to spread the lipid inks homogeneously and thinly. The polymer pen array (stamp) was glued onto a microscopy slide and mounted onto the tip holder. Two different pattern designs were used in this study. For the size gradient patterns, first an approach dot was patterned, to check the parallel alignment of stamp and substrate (levelling).[26,28] Subsequently, the pen array was tilted by ∼0.03° with respect to the substrate with the internal controls of the printing setup. A detailed introduction to the procedure of tilted stamp PPL was published elsewhere.[50,53] To allow for statistical average, a 3 × 3 dot scheme, each dot printed with a dwell time of 3 s was patterned at 70%RH. For the density gradient pattern, a 1 × 2 matrix was patterned manually (i.e., by positioning the stamp in x−y position by moving it appropriate distances in the control software, then letting the stamp approach the surface by the distance predefined in the alignment process, and after 3 s retracting the stamp for the same distance before navigating to the next x−y position to be patterned) with each step as shown in Scheme 1b at 50% RH. All RHs were fixed during the experiments and controlled within ±1%.

Protein Binding Experiment. Gradient patterns were generated as described above with a DOPC ink mixed by 5 mol % Biotin-PE to introduce functional protein binding sites. After writing the biotin-lipid ink in the same procedure as for the fluorescent ink pattern, the samples were incubated with 10% (w/V) bovine serum albumin (BSA) in phosphate buffered saline (PBS) for 10 min for blocking to avoid unspecific binding, followed by incubation 1% (v/v) of cy3-labeled streptavidin in PBS for 10 min. Afterward samples were analysed by fluorescence microscopy.

Optical Microscopy. The fluorescently labelled surface patterns were imaged by an upright fluorescence microscope (Eclipse 80i, Nikon), equipped with a sensitive camera (CoolSNAP HQ2, Photometrics), a broadband excitation light source (Intensilight, Nikon), and a Texas Red filter set (Y-2E/C, Nikon). SEEC microscopy54,55 (SARFUS 3D-AIR setup, Nanolane), which can provide information on lipid membrane structural height and stacking down to 1.5 nm height,[38] was done on samples with doped and undoped lipid structures on SiO_2 SURF substrates. Samples can be imaged fast (in comparison to atomic force microscopy (AFM)) with this technique, allowing for a picture of the membrane layered structures right after the printing process over the full areas of the substrates.

Contact Angle Measurements. Static contact angles for glass and SiO_2 SURF substrates were measured using an OCA-20 contact angle meter from DataPhysics Instruments GmbH. Glass samples were cleaned by sonicating with chloroform, isopropanol, and water each for 5 min. The SiO2 SURF samples were used directly after peeling the protective layer. The static contact angles of the samples were recorded at room temperature. For each measurement, three to four water droplets (meaning three or four measurements) with the same volume and rate (2 µL, 2 µL/min) were dropped on the surface and the average value of contact angle was reported.

Atomic Force Microscopy. For a high-resolution, detailed characterization of some representative features of the patterns on several samples, AFM was employed either on a Dimension Icon (Bruker, Germany) or on an MFP-3D-BIO AFM system (Asylum Research, USA) in tapping mode with HQ:NSC15/Al BS cantilevers (MikroMasch, USA) with 325 kHz nominal resonance frequency. All measurements were done in air under ambient conditions. Image processing and export was carried out in the respectively onboard software packages and WSxM.56 The roughness measurements were done on the Dimension Icon setup equipped with the same cantilevers as for imaging. The root-mean-square (RMS) average of height deviations with regard to the mean image data plane (Rq in the software) was extracted from 3 × 3 μm^2 images with the on-board software.

Image Analysis. The software ImageJ2[57] in the Bio7[58] distribution was used for the perimeter to area ratio analysis. First, the AFM images were converted to 8-bit greyscale and thresholded in ImageJ2 canvas. Then, the "Analyze Particles⋯" tool was used to extract perimeter length l and area A values. The ratio l/A was then calculated for each feature and used in the analysis; all calculations and measurements were done in pixels.

RESULTS AND DISCUSSION

First, feature size gradients were generated by implementing the strategy of tilted PPL stamps: after careful alignment of the PPL stamp parallel to the printing substrate, an intentional tilt of 0.03° was introduced,[50] leading to a gradient in contact pressure of the individual pens along

the 5 mm × 5mm dimensions of stamp size. A typical outcome of such a printing procedure is shown in Figure 1.

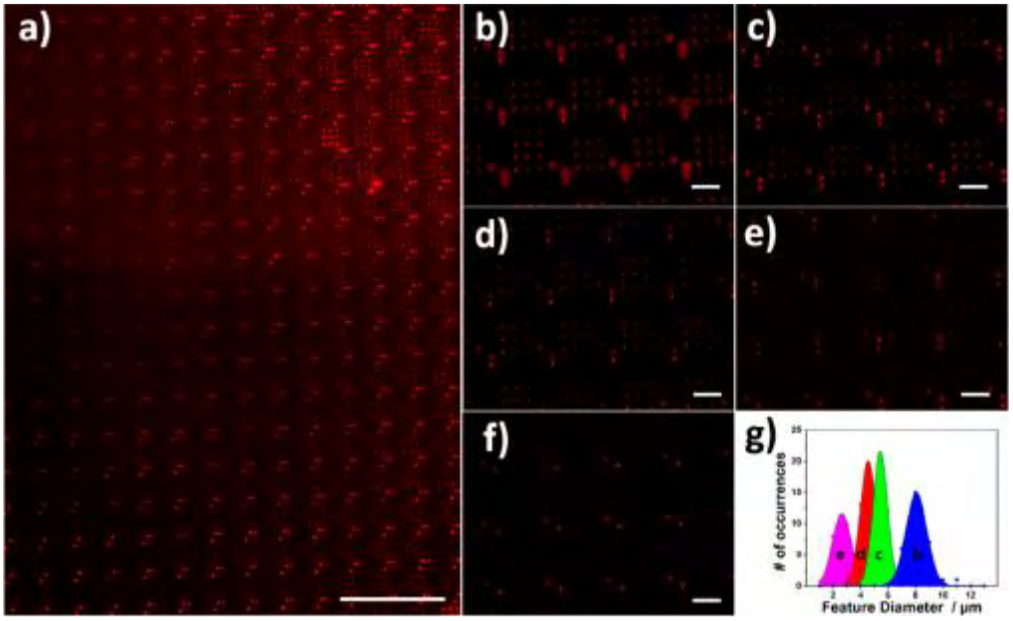

Figure 1. Fluorescence images from a feature size gradient on glass. (a) Overview image of the central part of the gradient pattern. Applied contact pressure is increasing from the bottom left to the top right. The overall gradient spans over 25 mm^2. Scale bar is 300 µm. (b–f) Higher magnification images of different positions along the feature size gradient. Scale bars are 50 µm. (g) Histogram of feature sizes in images (b) to (e).

The overview image in Figure 1a (approx. 1.3 mm × 1.7 mm area) shows the central area of the feature size gradient with neatly decreasing feature size from top right to bottom left corresponding to decreased contact pressure, in agreement with reports of molecular inks.[18,41,59] The overall feature size within the whole gradient pattern (spanning a whole 5 mm × 5mmas defined by the stamp size) varies from 7.6 ± 0.8 µm to 2.3 ± 0.6 µm. To obtain exact data on feature size and height, AFM was performed on different parts of the patterns.

In conjunction with the glass substrates, also SiO_2 SURF substrates, commercially available substrates with a hydroxylized silicon oxide surface and a layer structure underneath optimized for ellipsometric microscopy (see methods and Supporting Information for more details) were used. Interestingly, the AFM showed profound differences in the shape of the features on glass surfaces and SiO_2 SURF substrates (Figure 2): on glass samples, the features have a rougher circumference than on the SiO_2 SURF samples.

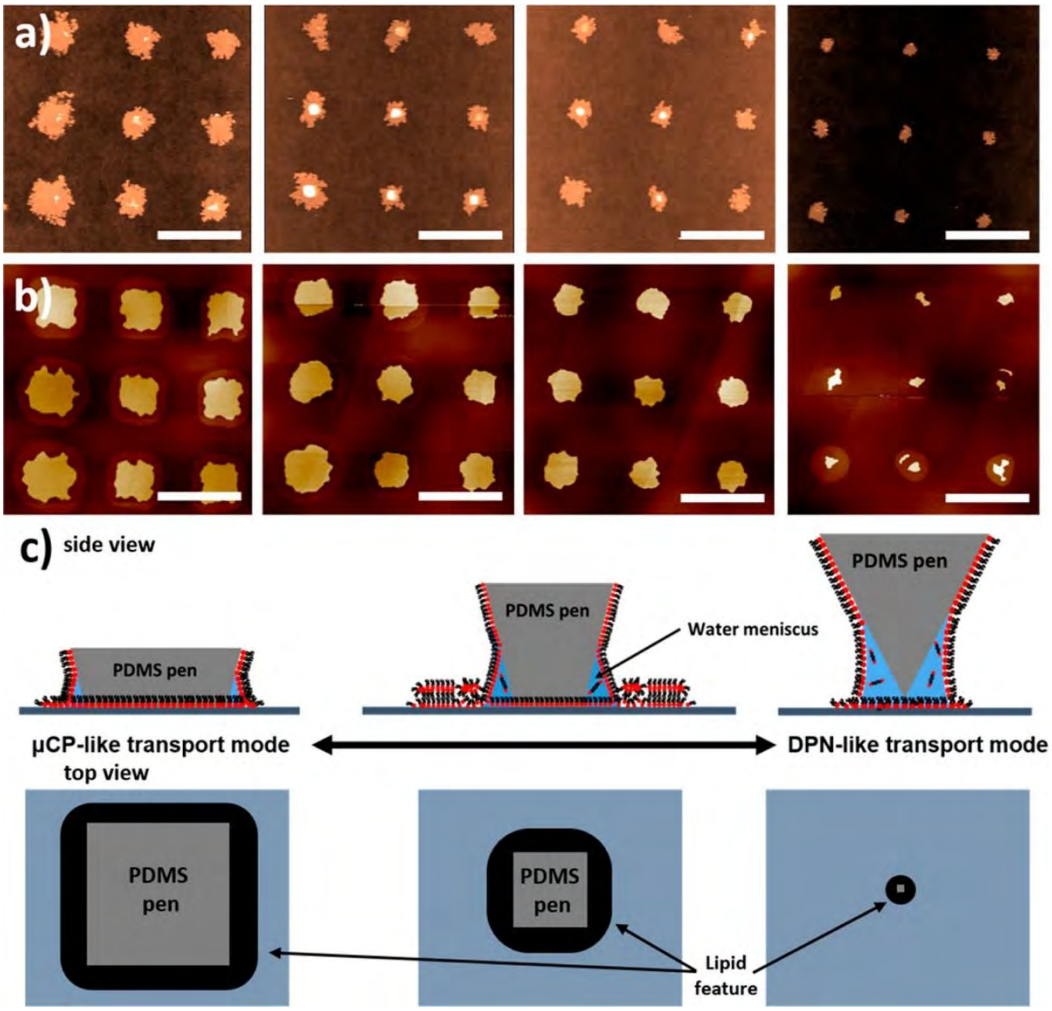

Figure 2. AFM characterization of the feature size gradients. AFM images of the feature size gradient at different positions along the gradient (a) on the glass substrates and (b) SiO_2 SURF substrates. Scale bars equal 20 μm. (c) Scheme of transfer modes for high, intermediate, and low contact pressure inside view (top row) and top view (bottom row). The lipid organization on the substrate (top row) and the resulting shape of the printed feature (bottom row) are shown.

This can be quantified by calculating the perimeter length to area ratio for the features, which average 237.2 ± 41.5 pixels−1 for glass compared to 123.4 ± 18.5 pixels−1 for the SiO_2 SURF, respectively, for the first three images presented in Figure 2 for each surface (the ones with the smallest features was excluded to prevent pixilation artifacts). Both surfaces are mildly hydrophilic (contact angle of 61.9 ± 3.3° for SiO_2 SURF and 45.3 ± 4.2° for glass, respectively), with a slightly smoother surface on the SiO_2 SURF (0.156 nm RMS) compared to glass (0.217 nm RMS). The higher surface roughness on glass potentially lowering the mobility in the membrane[60,61] seems to induce the anomalous surface diffusion on the glass. On hydrophobic surfaces, very flat surfaces like graphene[32] also show distinctive differences in spreading to hydrophobic self-assembled monolayers[62] or polymer surfaces.[63] On both surfaces, features appear more square-like the higher the contact pressure gets. This indicates the transition from a mainly DPN-like mode that is best described as surface diffusion of the lipid membrane from

a point source, resulting in round features, to a more µCP-like mode, where the lipids are instead stamped to the surface and diffusion plays only a minor role compared to the main area of the features at the edges of the deformed pen apex. The square-like deformation of the pen apexes is here translated into the shape of the resulting lipid membrane feature.

This switch in printing mode is also influenced by the surface type. When comparing feature height and area within the gradient on glass and SiO_2 SURF substrates different behaviours are observed: While for the glass samples, feature height increases as contact pressures increases up to a certain point, after which the height starts decreasing, it stays constant for all features on the SiO_2 SURF substrates (Figure 3a). At the same time, feature area increases with increasing pressure for both surfaces with similar rate (Figure 3b). The overall delivered ink volume per feature (Figure 3d) follows the combined trend of feature area and height, and so is continuously increasing with pressure in the SiO_2 SURFs but reaching a maximum at middle range pressure for the glass substrates.

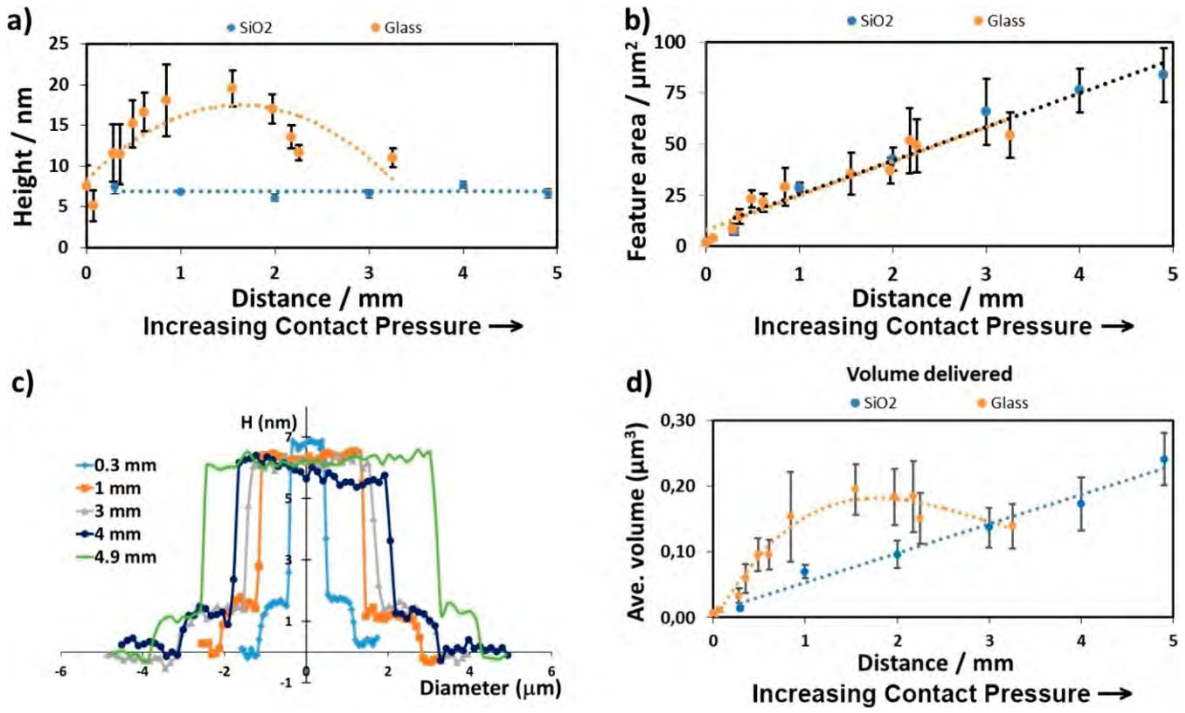

Figure 3. Quantification of the feature topography in a feature size gradient sample as shown in Figure 1. (a) Feature height and (b) feature area along the gradient for standard glass and SiO_2 SURF sample. (c) AFM profile lines of features along the gradient on the SiO_2 SURF sample. (d) Average ink volume delivered to the sample within a feature. The x-axis in (a), (b), and (d) give the distance along a straight line from gradient pattern start (low pressure) to the end of the gradient pattern (high pressure).

It should be noted that even though significant lipid volume is transferred in each feature, no ink depletion is occurring at the pen apexes, as ink can re-flow from the pen base and the stamp area located between the pens acts as ink reservoir. It was reported previously that no depletion occurs for at least up to 100 printed features.[26] The height of the features on the SiO_2 SURF samples is about 7 nm and compatible with two bilayers of lipids and a wetting (mono)layer underneath (Figure 3c). These layer heights and the implied layer organization are in agreement

with previous results for DPN deposited membranes and molecular dynamics simulations.[31,38,64,65] Overall, this suggests, in addition to the pressure induced switch between more DPN-like and μCP-like transfer mode, that the change in pen shape also likely influences the hydration state of the lipids due to the accompanying change in meniscus, which strongly influences viscosity and transfer behaviour of the lipid ink.[39,40,66] At lower contact pressure and DPN-like transport characteristics, the lipids (or hydrated lipid ink mixture) transport through the meniscus and fast surface spreading leads to flat and uniform membrane structures. At higher pressure, when ink transport mode switches to a μCP-like regime, the water meniscus volume at the rim of the deformed pen apex starts decreasing relative to the area directly under the deformed pen apex (eventually, at some point there is no free water anymore between deformed pen and substrate), and lipid molecules transfer mainly (in regard to feature area) at the contact area of the deformed pens. The remaining meniscus at the rim of the deformed pen apex leads to rounded edges of the otherwise now mainly square-shaped features. When less water is available for the hydration of the lipid ink, the surface spreading is hindered by increased viscosity,[39] leading to the rise of feature height. Because in the more μCP-like transfer mode the deformed pen apex blocks ever-increasing parts of the feature from free transfer of lipids, this rise can only increase up to a certain threshold, after which feature height starts decreasing again, as most material is now redistributing to fill the hole left in the middle of the feature, where transfer was blocked (Figure 4).

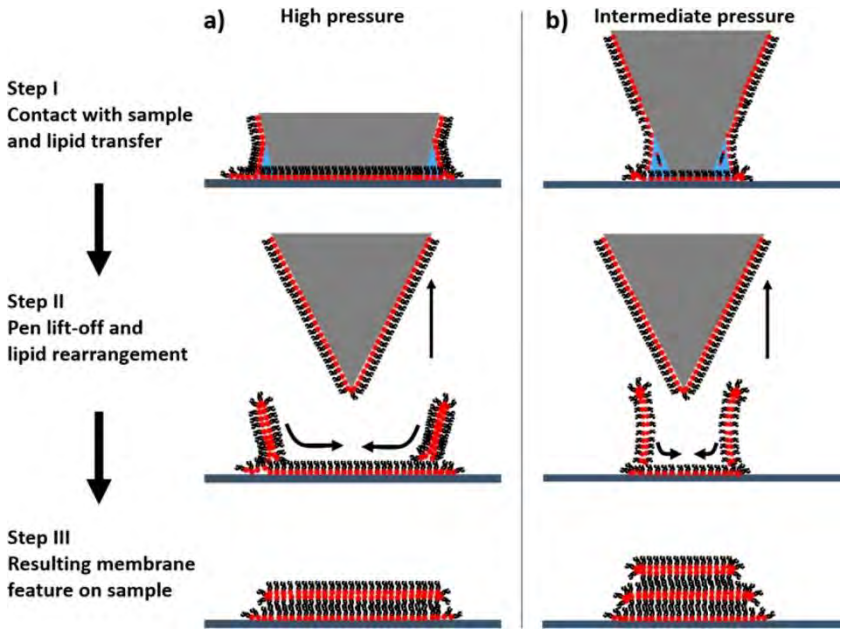

Figure 4. Scheme on high and intermediate pressure lipid transfer on glass. The deformation of the pen apex at high pressure (a) leaves a hole in the feature which is filled by spreading and lipid reconfiguration upon stamp retraction. However, in the intermediate pressure case (b) the deformation and resulting hole is smaller, which can lead to smaller but higher features in the intermediate pressure regime.

In contrast, on the SiO_2 SURF substrate, feature height stays constant, as the increased viscosity of the lipid ink that hinders spreading in the glass case is now compensated by the more homogeneous surface spreading. The role of surface spreading can also be seen within a single

printed gradient by overloading the stamp with ink before printing, leading to a much higher lipid transfer (Figure S2).

Here, so much lipid ink is transferred to the substrate, that at the higher-pressure regions, the wetting monolayers (interfacing the hydrophilic substrate with the membrane stacks above it) of neighbouring features are actually merging, resulting in a continuous layer that is essentially now a hydrophobic substrate to print on. While highly hydrophobic and atomically flat substrates like graphene strongly promote lipid spreading,[31,32] mildly hydrophobic and comparably rough surfaces as the hydrocarbon chains rather keep the membranes stacked on them in place.[62] On the now hydrophobic, high-pressure parts of the sample, much higher features even approaching drop-like profiles can be observed, while on the low-pressure parts, where still enough substrate area is open to allow spreading, flat membrane stacks are prevailing (Figure S3). Another effect of the increased ink flow is the suppression of the µCP-like transfer mode. Even in the highest-pressure part of the substrate, feature circumferences remain rounded in shape. Another interesting feature species can be observed when membrane spreading is not dominant (i.e., on glass samples) and high pressure is applied. Here, one can see that the rearrangement of the lipid is rather quick and sometimes already occurs during the retraction of the pen array, while the pen/meniscus is still in contact with the structures, as is evident by remaining x-shaped structures on top of some of the features (Figure S4).

After having established the transfer characteristics for feature size gradients, we explored the feasibility of creating a feature density gradient by printing lipids via PPL. To obtain a large area feature density gradient as shown in Figure 5, 0.5 × 0.5 cm^2 stamps were inked with a fluorescently labelled lipid mixture and stamped onto the substrates in the following writing strategy. The first subpatterns were generated as in a standard PPL print (left side of Figure 5), but then, the whole pen array was shifted by 1 mm in the x-axis. In the next round of printing, the additional set of subpatterns were created, while the left 1 × 5mm^2 area of the previously patterned area remained unaltered. Subsequently, by repeating this printing scheme, the pen array generated the feature density gradient over the entire area as seen in Figure 5. Here, a uniform feature diameter of 3.6 ± 0.5 µm was observed over the whole pattern, with exception of some outliers with much larger sizes in the range 6 to 9 µm. These were probably caused by fluctuations in ink flow during the manual printing process.

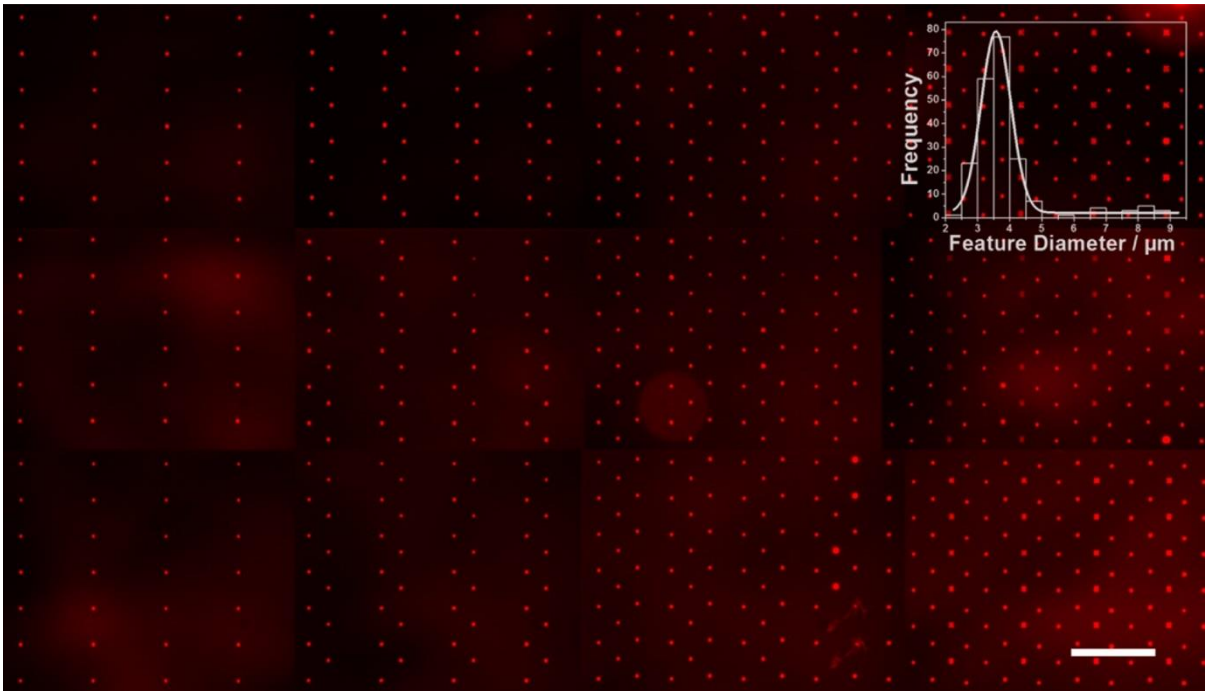

Figure 5. Feature density gradient. The composite overview of 12 fluorescence microscopy images taken from the feature density gradient generated with fluorescently labelled lipid ink. Scale bar is 100 µm. The inset shows the feature diameter distribution throughout the area.

To demonstrate that the gradient lipid pattern can be further functionalized, e.g., for use in protein presentation,[3] we generated a bioactive feature size gradient pattern. For this, the lipid ink without any fluorescent labelling was doped with a modified lipid, bearing a biotin moiety on its headgroup. First, the resulting pattern is not observable in fluorescence. Lipid patterns written by L-DPN are generally stable over prolonged time periods in air when not exposed to high humidity,[63] and can easily be transferred into liquid phase for experiments with several washing steps[63,67,68] or even used in cell culture conditions.[34,35] The lipid printed by PPL exhibits a similar quality: to demonstrate selective protein binding, such a prepared gradient pattern was incubated (after appropriate blocking steps) with a solution of fluorescently labelled streptavidin. As streptavidin shows a high affinity for biotin,[69] it will self-assemble on the biotin bearing lipid pattern and make the pattern fluorescent. Figure 6 shows a typical image of a PPL printed biotin−lipid gradient pattern after the incubation procedure. The pattern now clearly emerges from the background due to the specific binding of the fluorescently labelled streptavidin.

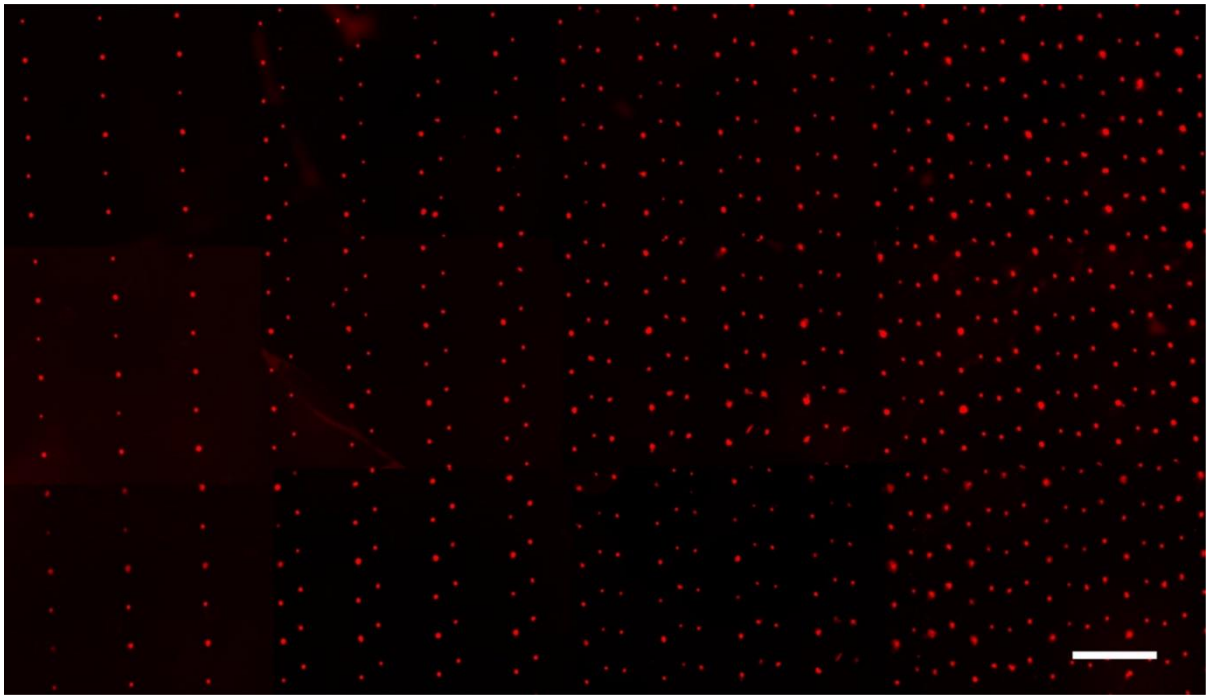

Figure 6. Protein decorated feature density gradient. The composite image consists of 12 fluorescence microscopy images taken from the biotin containing feature density gradient after incubation with streptavidin-cy3. Scale bar equals 100 µm.

As streptavidin can be used as a generic linker to other biotin-labeled proteins, this strategy can generate arbitrary gradient patterns of, e.g., antibodies for screening applications or signaling proteins for assays in cell culture experiments, as L-DPN and PPL lipid patterns were already demonstrated to be stable enough for cell culture conditions,[3,34,35] or use in protein crystallization assays.[67]

CONCLUSSIONS

PPL can be employed to generate several square millimetres spanning lipid feature gradients varying in feature size and density. Two different transfer modes in PPL with lipids were observed, one more resembling L-DPN and the other µCP. The switch between these transfer modes is dependent on the applied contact pressure, while the printing results in regard to feature height are modulated additionally by the substrate type. For SiO_2 SURF substrates, constant height features with an area size gradient can be fabricated independently of the contact pressure on the specific pens, while on standard glass coverslips additional variation in feature height over the course of the gradient can be obtained. The ability of transfer mode selection arises thanks to the particular attributes of phospholipids, as compared to molecular inks, concerning their assembly and spreading behaviour. Ultimately, choosing the right printing parameters, along with a controlled inking procedure resulting in a homogeneously thin lipid ink coverage on the PPL stamp, allows full control on the ink transport, being capable of printing membrane like structures of different lateral sizes while having a height resembling biological membranes. These lipid membrane patterns could be useful for gradient presentation of functional lipid mixtures or in experiments on lipid membrane organization. By introducing biotin-bearing lipids into the ink, proteins can be selectively immobilized on the lipid gradient

pattern. More complicated sandwich systems can be constructed over streptavidin conjugation, allowing virtually free choice of protein (or other biotinylated compounds) for presentation on the pattern. Therefore, the resulting gradient patterns enable many experimental options for experiments in cell signalling and cell migration assays.

ACKNOWLEDGEMENTS

This work was carried out with the support of the Karlsruhe Nano Micro Facility (KNMF, www.kmf.kit.edu), a Helmholtz Research Infrastructure at Karlsruhe Institute of Technology (KIT, www.kit.edu). A.U. acknowledges the People Programme (Marie Curie Actions) of the European Union's Seventh Framework Programme FP7/2007-2013 under REA grant agreement no. 328163. S.G. thanks the DAAD for support in form of a WISE grant (WISE 2016 57220756). Q. R. thanks the Karlsruhe House of Young Scientist (KHYS) for support in form of a KIT internship grant. S.L. acknowledges funding from the NIH (R01 GM107172).

Corresponding Author: michael.hirtz@kit.edu

REFERENCES

(1) Greiner, A. M.; Sales, A.; Chen, H.; Biela, S. A.; Kaufmann, D.; Kemkemer, R. Nano- and Microstructured Materials for in Vitro Studies of the Physiology of Vascular Cells. Beilstein J. Nanotechnol. 2016, 7, 1620−1641.

(2) Satav, T.; Huskens, J.; Jonkheijm, P. Effects of Variations in Ligand Density on Cell Signaling. Small 2015, 11, 5184−5199.

(3) Sekula, S.; Fuchs, J.; Weg-Remers, S.; Nagel, P.; Schuppler, S.; Fragala, J.; Theilacker, N.; Franzreb, M.; Wingren, C.; Ellmark, P.; et al. Multiplexed Lipid Dip-Pen Nanolithography on Subcellular Scales for the Templating of Functional Proteins and Cell Culture. Small 2008, 4, 1785−1793.

(4) Liu, W.-D.; Yang, B. Patterned Surfaces for Biological Applications: A New Platform Using Two Dimensional Structures as Biomaterials. Chin. Chem. Lett. 2017, 28, 675−690.

(5) Shah, S.; Solanki, A.; Lee, K.-B. Nanotechnology-Based Approaches for Guiding Neural Regeneration. Acc. Chem. Res. 2016, 49,17−26.

(6) Tjong, V.; Tang, L.; Zauscher, S.; Chilkoti, A. Smart" DNA Interfaces. Chem. Soc. Rev. 2014, 43, 1612−1626.

(7) Malmström, J.; Travas-Sejdic, J. Orthogonal Surface Function-alization through Bioactive Vapor-Based Polymer Coatings. J. Appl. Polym. Sci. 2014, 131,1−12.

(8) Genzer, J.; Bhat, R. R. Surface-Bound Soft Matter Gradients. Langmuir 2008, 24, 2294−2317.

(9) Nicosia, C.; Huskens, J. Reactive Self-Assembled Monolayers: From Surface Functionalization to Gradient Formation. Mater. Horiz. 2014, 1,32−45.

(10) You, C.; Piehler, J. Functional Protein Micropatterning for Drug Design and Discovery. Expert Opin. Drug Discovery 2016, 441,1−15.

(11) Wan, P.; Xing, Y.; Chen, Y.; Chi, L.; Zhang, X. Host−guest Chemistry at Interface for Photoswitchable Bioelectrocatalysis. Chem. Commun. 2011, 47, 5994.

(12) Wan, P.; Chen, X. Stimuli-Responsive Supramolecular Interfaces for Controllable Bioelectrocatalysis. ChemElectroChem 2014, 1, 1602− 1612.

(13) Luo, C. S.; Wan, P.; Yang, H.; Shah, S. A. A.; Chen, X. Healable Transparent Electronic Devices. Adv. Funct. Mater. 2017, 27, 1606339.

(14) Ross, A. M.; Lahann, J. Surface Engineering the Cellular Microenvironment via Patterning and Gradients. J. Polym. Sci., Part B: Polym. Phys. 2013, 51, 775−794.

(15) Lagunas, A.; Martínez, E.; Samitier, J. Surface-Bound Molecular Gradients for the High-Throughput Screening of Cell Responses. Front. Bioeng. Biotechnol. 2015, 3,1−6.

(16) Hickman, G. J.; Boocock, D. J.; Pockley, A. G.; Perry, C. C. The Importance and Clinical Relevance of Surfaces in Tissue Culture. ACS Biomater. Sci. Eng. 2016, 2, 152−164.

(17) van Weerd, J.; Karperien, M.; Jonkheijm, P. Supported Lipid Bilayers for the Generation of Dynamic Cell-Material Interfaces. Adv. Healthcare Mater. 2015, 4, 2743−2779.

(18) Huo, F.; Zheng, Z.; Zheng, G.; Giam, L. R.; Zhang, H.; Mirkin, C.A. Polymer Pen Lithography. Science 2008, 321, 1658−1660.

(19) Piner, R. D.; Zhu, J.; Xu, F.; Hong, S.; Mirkin, C. A. Dip-Pen" Nanolithography. Science 1999, 283, 661−663.

(20) Xia, Y.; Whitesides, G. M. Soft Lithography. Angew. Chem., Int. Ed. 1998, 37, 550−575.

(21) Hong, J. M.; Ozkeskin, F. M.; Zou, J. A Micromachined Elastomeric Tip Array for Contact Printing with Variable Dot Size and Density. J. Micromech. Microeng. 2008, 18, 15003.

(22) Jang, J.-W.; Smetana, A.; Stiles, P. Multi-Ink Pattern Generation by Dip-Pen Nanolithography. Scanning 2010, 32,24−29.

(23) Collins, J. M.; Nettikadan, S. Sub-Cellular Scaled Multiplexed Protein Patterns for Single Cell Cocultures. Anal. Biochem. 2011, 419, 339-341.

(24) Martínez-Otero, A.; González-Monje,P.;Maspoch,D.; Hernando, J.; Ruiz-Molina, D. Multiplexed Arrays of Chemosensors by Parallel Dip-Pen Nanolithography. Chem. Commun. 2011, 47, 6864.

(25) Zheng, Z.; Daniel, W. L.; Giam, L. R.; Huo, F.; Senesi, A. J.; Zheng, G.; Mirkin, C. A. Multiplexed Protein Arrays Enabled by Polymer Pen Lithography: Addressing the Inking Challenge. Angew. Chem., Int. Ed. 2009, 48, 7626−7629.

(26) Brinkmann, F.; Hirtz, M.; Greiner, A. M.; Weschenfelder, M.; Waterkotte, B.; Bastmeyer, M.; Fuchs, H. Interdigitated Multicolored Bioink Micropatterns by Multiplexed Polymer Pen Lithography. Small 2013, 9, 3266−3275.

(27) Arrabito, G.; Schroeder, H.; Schröder, K.; Filips, C.; Marggraf, U.; Dopp, C.; Venkatachalapathy, M.; Dehmelt, L.; Bastiaens, P. I. H.; Neyer, A.; et al. Configurable Low-Cost Plotter Device for Fabrication of Multi-Color Sub-Cellular Scale Microarrays. Small 2014, 10, 2870− 2876.

(28) Kumar, R.; Weigel, S.; Meyer, R.; Niemeyer, C. M.; Fuchs, H.; Hirtz, M. Multi-Color Polymer Pen Lithography for Oligonucleotide Arrays. Chem. Commun. 2016, 52, 12310−12313.

(29) Lenhert, S.; Sun, P.; Wang, Y.; Fuchs, H.; Mirkin, C. A. Massively Parallel Dip-Pen Nanolithography of Heterogeneous Supported Phospholipid Multilayer Patterns. Small 2007, 3,71−75.

(30) Bog, U.; Laue, T.; Grossmann, T.; Beck, T.; Wienhold, T.; Richter, B.; Hirtz, M.; Fuchs, H.; Kalt, H.; Mappes, T. On-Chip Microlasers for Biomolecular Detection via Highly Localized Deposition of a Multifunctional Phospholipid Ink. Lab Chip 2013, 13, 2701−2707.

(31) Hirtz, M.; Oikonomou, A.; Georgiou, T.; Fuchs, H.; Vijayaraghavan, A. Multiplexed Biomimetic Lipid Membranes on Graphene by Dip-Pen Nanolithography. Nat. Commun. 2013, 4, 2591.

(32) Hirtz, M.; Oikonomou, A.; Clark, N.; Kim, Y.-J.; Fuchs, H.; Vijayaraghavan, A. Self-Limiting Multiplexed Assembly of Lipid Membranes on Large-Area Graphene Sensor Arrays. Nanoscale 2016, 8, 15147−15151.

(33) Rath, P.; Hirtz, M.; Lewes-Malandrakis, G.; Brink, D.; Nebel, C.; Pernice, W. H. P. Diamond Nanophotonic Circuits Functionalized by Dip-Pen Nanolithography. Adv. Opt. Mater. 2015, 3, 328−335.

(34) Sekula-Neuner, S.; Maier, J.; Oppong, E.; Cato, A. C. B.; Hirtz, M.; Fuchs, H. Allergen Arrays for Antibody Screening and Immune Cell Activation Profiling Generated by Parallel Lipid Dip-Pen Nanolithography. Small 2012, 8, 585−591.

(35) Oppong, E.; Hedde, P. N.; Sekula-Neuner, S.; Yang, L.; Brinkmann, F.; Dörlich, R. M.; Hirtz, M.; Fuchs, H.; Nienhaus, G. U.; Cato, A. C. B. Localization and Dynamics of Glucocorticoid Receptor at the Plasma Membrane of Activated Mast Cells. Small 2014, 10, 1991-1998.

(36) Hirtz, M.; Sekula-Neuner, S.; Urtizberea, A.; Fuchs, H. Functional Lipid Assemblies by Dip-Pen Nanolithography and Polymer Pen Lithography. In Soft Matter Nanotechnology: From Structure to Function, Chen, X.; Fuchs, H., Eds.; Wiley-VCH Verlag GmbH & Co. KGaA: Weinheim, Germany, 2016; pp 161−186.

(37) Biswas, S.; Brinkmann, F.; Hirtz, M.; Fuchs, H. Patterning of Quantum Dots by Dip-Pen and Polymer Pen Nanolithography. Nanofabrication 2015, 2,19−26.

(38) Hirtz, M.; Corso, R.; Sekula-Neuner, S.; Fuchs, H. Comparative Height Measurements of Dip-Pen Nanolithography-Produced Lipid Membrane Stacks with Atomic Force, Fluorescence, and Surface Enhanced Ellipsometric Contrast Microscopy. Langmuir 2011, 27, 11605−11608.

(39) Urtizberea, A.; Hirtz, M. A Diffusive Ink Transport Model for Lipid Dip-Pen Nanolithography. Nanoscale 2015, 7, 15618−15634.

(40) Urtizberea, A.; Hirtz, M.; Fuchs, H. Ink Transport Modelling in Dip-Pen Nanolithography and Polymer Pen Lithography. Nano-fabrication 2015, 2,43−53.

(41) Liao, X.; Braunschweig, A. B.; Zheng, Z.; Mirkin, C. A. Force-and Time-Dependent Feature Size and Shape Control in Molecular Printing via Polymer-Pen Lithography. Small 2010, 6, 1082−1086.

(42) Giam, L. R.; Wang, Y.; Mirkin, C. A. Nanoscale Molecular Transport: The Case of Dip-Pen Nanolithography. J. Phys. Chem. A 2009, 113, 3779−3782.

(43) Stifter, T.; Marti, O.; Bhushan, B. Theoretical Investigation of the Distance Dependence of Capillary and van Der Waals Forces in Scanning Force Microscopy. Phys. Rev. B: Condens. Matter Mater. Phys. 2000, 62, 13667−13673.

(44) Kim, H.; Smit, B.; Jang, J. Monte Carlo Study on the Water Meniscus Condensation and Capillary Force in Atomic Force Microscopy. J. Phys. Chem. C 2012, 116, 21923−21931.

(45) Jang, J.; Schatz, G. C.; Ratner, M. A. Liquid Meniscus Condensation in Dip-Pen Nanolithography. J. Chem. Phys. 2002, 116, 3875−3886.

(46) Lenhert, S.; Mirkin, C. A.; Fuchs, H. In Situ Lipid Dip-Pen Nanolithography under Water. Scanning 2010, 32,15−23.

(47) Rozhok, S.; Sun, P.; Piner, R.; Lieberman, M.; Mirkin, C. A. AFM Study of Water Meniscus Formation between an AFM Tip and NaCl Substrate. J. Phys. Chem. B 2004, 108, 7814−7819.

(48) Peterson, E. J.; Weeks, B. L.; De Yoreo, J. J.; Schwartz, P. V. Effect of Environmental Conditions on Dip Pen Nanolithography of Mercaptohexadecanoic Acid. J. Phys. Chem. B 2004, 108, 15206− 15210.

(49) Schwartz, J. J.; Hohman, J. N.; Morin, E. I.; Weiss, P. S. Molecular Flux Dependence of Chemical Patterning by Microcontact Printing. ACS Appl. Mater. Interfaces 2013, 5, 10310−10316.

(50) Giam, L. R.; Massich, M. D.; Hao, L.; Shin Wong, L.; Mader, C. C.; Mirkin, C. A. Scanning Probe-Enabled Nanocombinatorics Define the Relationship between Fibronectin Feature Size and Stem Cell Fate. Proc. Natl. Acad. Sci. U. S. A. 2012, 109, 4377−4382.

(51) Ulrich, A. S.; Sami, M.; Watts, A. Hydration of DOPC Bilayers by Differential Scanning Calorimetry. Biochim. Biophys. Acta, Biomembr. 1994, 1191, 225−230.

(52) Filippov, A.; Orädd, G.; Lindblom, G. Influence of Cholesterol and Water Content on Phospholipid Lateral Diffusion in Bilayers. Langmuir 2003, 19, 6397−6400.

(53) Eichelsdoerfer, D. J.; Liao, X.; Cabezas, M. D.; Morris, W.; Radha, B.; Brown, K. A.; Giam, L. R.; Braunschweig, A. B.; Mirkin, C. A. Large-Area Molecular Patterning with Polymer Pen Lithography. Nat. Protoc. 2013, 8, 2548−2560.

(54) Ausserré, D.; Valignat, M.-P. Wide-Field Optical Imaging of Surface Nanostructures. Nano Lett. 2006, 6, 1384−1388.

(55) Ausserré, D.; Valignat, M.-P. Surface Enhanced Ellipsometric Contrast (SEEC) Basic Theory and lambda/4 Multilayered Solutions. Opt. Express 2007, 15, 8329−8339.

(56) Horcas, I.; Fernández, R.; Gómez-Rodríguez, J. M.; Colchero, J.; Gómez-Herrero, J.; Baro, A. M. WSXM: A Software for Scanning Probe Microscopy and a Tool for Nanotechnology. Rev. Sci. Instrum. 2007, 78, 13705.

(57) Schindelin, J.; Rueden, C. T.; Hiner, M. C.; Eliceiri, K. W. The ImageJ Ecosystem: An Open Platform for Biomedical Image Analysis. Mol. Reprod. Dev. 2015, 82, 518−529.

(58) Austenfeld, M.; Beyschlag, W. A Graphical User Interface for R in a Rich Client Platform for Ecological Modeling. J. Stat. Softw. 2012, 49,1 DOI: 10.18637/jss.v049.i04.

(59) Liao, X.; Braunschweig, A. B.; Mirkin, C. A. Force-Feedback" leveling of Massively Parallel Arrays in Polymer Pen Lithography. Nano Lett. 2010, 10, 1335−1340.

(60) Nissen, J.; Jacobs, K.; Rädler, J. O. Interface Dynamics of Lipid Membrane Spreading on Solid Surfaces. Phys. Rev. Lett. 2001, 86, 1904−1907.

(61) Blachon, F.; Harb, F.; Munteanu, B.; Piednoir, A.; Fulcrand, R.; Charitat, T.; Fragneto, G.; Pierre-Louis, O.; Tinland, B.; Rieu, J.-P. Nanoroughness Strongly Impacts Lipid Mobility in Supported Membranes. Langmuir 2017, 33, 2444−2453.

(62) Gavutis, M.; Navikas, V.; Rakickas, T.; Vaitekonis, Š.; Valiokas, R. Lipid Dip-Pen Nanolithography on Self-Assembled Monolayers. J. Micromech. Microeng. 2016, 26, 25016.

(63) Lenhert, S.; Brinkmann, F.; Laue, T.; Walheim, S.; Vannahme, C.; Klinkhammer, S.; Xu, M.; Sekula, S.; Mappes, T.; Schimmel, T.; et al. Lipid Multilayer Gratings. Nat. Nanotechnol. 2010, 5, 275−279.

(64) Willems, N.; Urtizberea, A.; Verre, A. F.; Iliut, M.; Lelimousin, M.; Hirtz, M.; Vijayaraghavan, A.; Sansom, M. S. P. Biomimetic Phospholipid Membrane Organization on Graphene and Graphene Oxide Surfaces: A Molecular Dynamics Simulation Study. ACS Nano 2017, 11, 1613−1625.

(65) Rivel, T.; Yesylevskyy, S. O.; Ramseyer, C. Structures of Single, Double and Triple Layers of Lipids Adsorbed on Graphene: Insights from All-Atom Molecular Dynamics Simulations. Carbon 2017, 118, 358−369.

(66) Rozhok, S.; Piner, R. D.; Mirkin, C. A. Dip-Pen Nano-lithography: What Controls Ink Transport? J. Phys. Chem. B 2003, 107, 751−757.

(67) Ielasi, F. S.; Hirtz, M.; Sekula-Neuner, S.; Laue, T.; Fuchs, H.; Willaert, R. G. Dip-Pen Nanolithography-Assisted Protein Crystal-lization. J. Am. Chem. Soc. 2015, 137, 154−157.

(68) Hirtz, M.; Brglez, J.; Fuchs, H.; Niemeyer, C. M. Selective Binding of DNA Origami on Biomimetic Lipid Patches. Small 2015, 11, 5752−5758.

(69) Wilchek, M.; Bayer, E. A. Introduction to Avidin-Biotin Technology. In Methods in Enzymology - Vol. 184: Avidin-Biotin Technology; Elsevier, 1990; pp 5−13.